Study of Additively Manufactured Channelized Ka-Band Metasurface Elements for Deployable Antennas

Blake A. Roberts, Cameron Martinez, Bryce Gray, John T. O'Keefe, Jayaprakash Shivakumar, and Eduardo Rojas Embry-Riddle Aeronautical University, Daytona Beach, FL 32114, USA, rojase1@erau.edu

Abstract—In recent years the market for small satellites have exponentially grown, which has resulted in rapid advancements in CubeSat compatible technologies. Deployable antennas offer a solution to achieve large antenna apertures, while allowing to stow the aperture during the launch process. This paper presents a novel deployment mechanism based on embedded dielectric thread, and studies the effects of this thread in the performance of the metasurface elements of the deployable antenna. The proposed hinge mechanism minimizes gaps created by traditional hinges, ensuring structural integrity and RF performance. Direct light processing is used to manufacture the channelized metasurface elements which are metalized using silver conductive pastes. Experimental results show that the channelized structure introduces minimal phase variation of 1.15% (1.92°) and 0.139 dB of added loss at 30 GHz, making it suitable for use with deployable reflectarrays in space applications. This work validates the usage of embedded channels in the dielectric of metasurface antennas, and presents results that can be used to adjust the antenna geometry to account for the effects of such channels.

Index Terms—Additive manufacturing, Origami, Origami Antennas, Ka-band, reflectarray, CubeSat, mm-wave

I. INTRODUCTION

Advancements in folding reflectarray antennas have allowed for compact high gain antennas to be used in cubesat applications. This is due to the fact that, unlike a parabolic reflector, a reflectarray can give high gain in a flat, easy to fold form factor [1]. A commonly used technique with reflectarray antennas is to take advantage of the flat sheet like structure and apply origami principles to allow for compact folding of such antennas into a size that accommodates compact launch requirements [2] [3] [4]. One common area of difficulty is the hinging mechanism. Unlike traditional origami paper, a reflectarray has an appreciable thickness, which leaves gaps that must be accounted for. It has been shown small gaps can be used at X-Band frequencies with minimal impact [5]. However, as there is a push into millimeter wave frequencies the gaps necessary for hinges may become significantly large. This paper proposes the use of additive manufacturing to create a channelized substrate that reduce gaps left by traditional hinges and explores the impacts of the channelized substrate on the performance of the reflectarray. The mechanism takes advantage of additive manufacturing to leave a path for a cable to run through the design as seen in Fig. 1a. When employing origami folding techniques on the panel it can be folded as normal, causing excess line to be drawn through the channels to accommodate these folds. Therefore, when the line is drawn

back in this shortens the line and results in the panel returning to its unfolded shape.

To validate the channelized design a single metasurface element is designed, manufactured, and measured. To generate the reflectarray design a process outlined in [6] is followed. The design of a single element for a reflectarray starts with selecting an element geometry that allows a reflection phase control from +180° to -180°. However, achieving a full 360° phase control is often challenging due to limitations imposed by the element's shape and geometry. In this design, a square element was chosen for its simplicity, which results in approximately 300° of phase. Each element consists of a metallic patch on a dielectric substrate, with its size varied to achieve the required phase shift for beam steering. The element parameters and corresponding phase response are used by an algorithm to generate the footprint of the entire array.

II. CHANNELIZED METASURFACE ELEMENT AND DEPLOYMENT MECHANISM DESIGN

A. Deployment Mechanism

By constructing a meandering channel that weaves twice through each edge of each mating face of every panel segment a cable is run through the channel as shown in Fig. 1. A centrally embedded pulley mechanism is used to tension the cable. As the extra cable is wound onto the reel, the panel edges are drawn together, causing the panels to unfold and align.

While this allows for nearly seamless alignment and gives rigidity to the open panel it does create a channel void of panel material. As a reflectarray relies on phasing between elements, it is necessary to investigate the impact of such channels.

To verify the reflectarray's robustness to this channel, a 2 element analysis is conducted using a WR-34. Two elements of the base element of the reflectarray design are placed an equal distance L from each other such that they evenly divide the space in the waveguide in a manner similar to [7]. Two versions of the design are made, one with the channel as seen in Fig. 2 and the other a baseline identical in all ways except without a channel in place. The dimensions used are h=1 mm, c=0.5 mm, L=4.318, g=0.684 mm, and p=2.95 mm. To simulate the design a floquet setup is employed inside of Ansys HFSS. Since a floquet port creates an infinite plane of its element, a single LxL element was used and can be seen in Fig. 3.

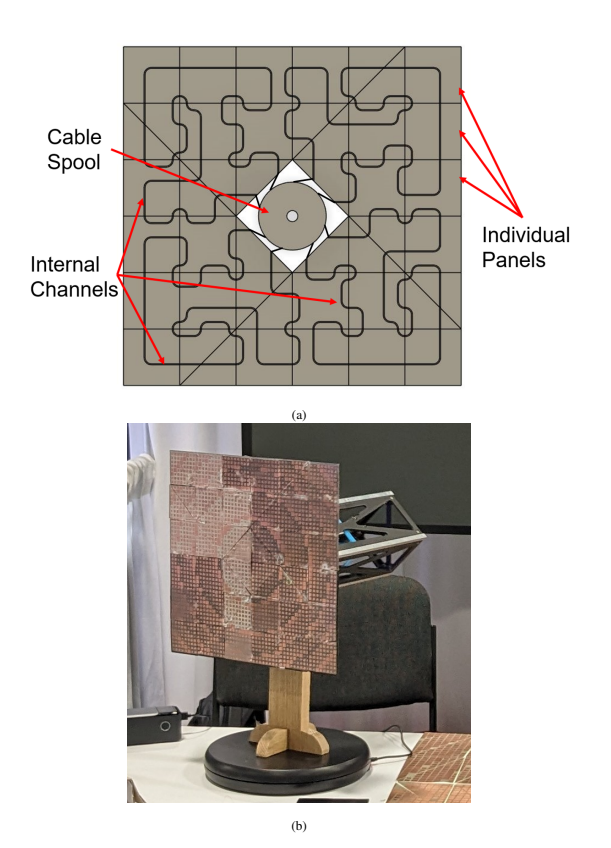


Fig. 1: Geometry of the deployable reflectarray. (a) Transparent 3D model showing the internal channels and the deployment mechanism. (b) Functional reflectarray prototype mounted on a 3U cubesat chasis.

Conductive Patch Ground Plane Channel with Kevlar Thread (a) 2L p (b) (c) ppective view of the two reflectarray cells sized for a size of the conductive patch.

Radix Substrate

Fig. 2: . (a) Perspective view of the two reflectarray cells sized for a WR-34 waveguide (b) top view of cells (C) side view of test sample with the Kevlar thread shown in brown.

B. Material Considerations

Additive manufacturing is a practical choice for this design as it would not be feasible to machine the channels in such a meandering pattern using subtractive manufacturing.

Digital light processing (DLP) printing is a process that uses UV-curable resins in conjunction with an LCD photomask to cure single layers of resin and build up a 3D structure. DLP printing is selected due to its ability to distinguish small feature sizes and achieve the detail needed for the design. Rogers Radix is selected for the substrate due to its comparable low loss (tan(δ)=0.0046 at 24 GHz) and favorable permittivity (ϵ r=2.8 at 24 GHz) [8] and its successful use in metasurface antennas [9]. For the experiment a poly(p-phenylene terephthalamide) (Kevlar) is due to its high temperature resistance and high tensile strength to size ratio.

III. ADDITIVE MANUFACTURING

The fabrication of the substrate is done using the Anycubic A5S Light Printing (DLP) printer using Rogers Radix resin. A layer height of 50 um is used with the cure time of 90 s. The first few layers of a resin print are over exposed to ensure adhesion to the build plate. To avoid any inconsistencies in print dimensions or material properties a support structure is used such that a removable raft is the section that is removed to ensure the sample is uniform. The raft can be seen in Fig. 4a.

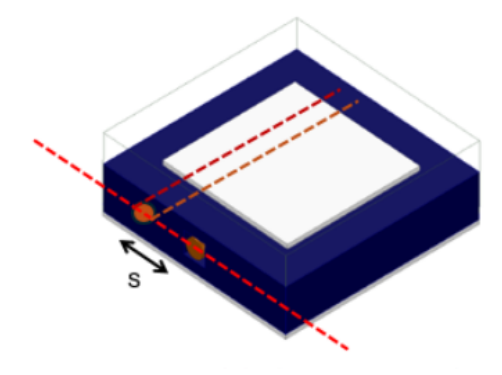


Fig. 3: Single reflectarray element geometry highlighting the channel offset (s).

The parts are then sonicated in 99% isopropyl alcohol for an hour to remove any excess resin. The supports are then carefully removed such that a small amount of excess is left to avoid any divots in the sample. Next, the parts are sanded to remove any extra material from the backside. The 3Dn-Tabletop is used to deposit DuPont CB028 onto the substrate forming the patches and the ground plane. A heat gun is used on the ground plane to ensure it is dry before flipping the part over to print the top patches. The parts are then baked at 90 °C for 60 min to cure the ink. The finished parts are shown in Fig. 4.



Fig. 4: Printed samples of Radix. Shown (a) with supports from printer, (b) with the baseline patches, and (c) with patches and a channel with Kevlar thread.

IV. MEASUREMENT SETUP

A Space Machines and Engineering coaxial to WR-34 waveguide adaptor is attached to a Keysight N5227B PNA Network Analyzer. The frequency sweep is set to 22 GHz to 32 GHz to cover the frequency range of the provided calkit. Calibration of the open ended waveguide is then performed with the Space Machines and Engineering WR-34 Calibration kit using a load, a quarter wavelength short, and a three eighths wavelength short. Each sample is loaded into a milled pocket to allow precise alignment and a good ground connection with the waveguide.

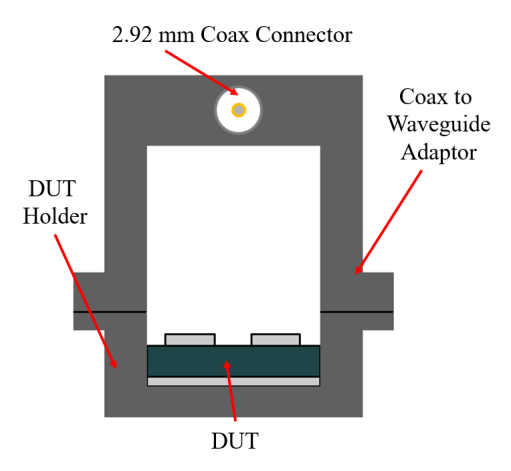
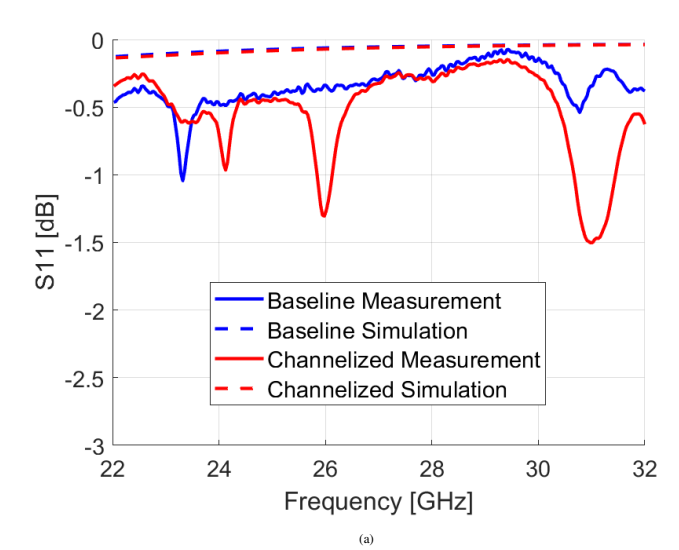


Fig. 5: Cross section of measurement set up including the coaxial to waveguide adapter, a DUT holder, and the RA elements.

V. RESULTS

The results in Fig. 6 show the variation in return loss and phase between the channelized and non-channelized samples. Table I shows the specific variations at the design frequency of 30 GHz. The measured data indicates that the phase variation is minimal, with only 1.92° difference at 30 GHz. This small phase variation suggests that the proposed hinge mechanism does not introduce significant phase changes in the patches.

In contrast, the variation in return loss shown in Fig. 6a is more pronounced; however, this variation is observed between the measurements and simulations rather than between the baseline and the channelized designs. The test setup could be sensitive to variation in the connection of the ground plane of the DUT and the test fixture. These small gaps could cause the peaks in reflection observed in the measurement that were



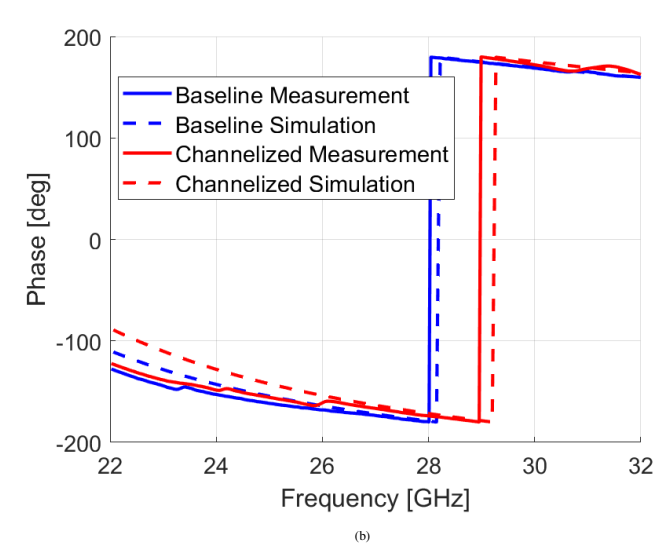


Fig. 6: Simulated and measured a) return loss and b) phase of samples with and without the channel.

not shown in simulation. However, table 1 does show only 0.139 db of added loss between the measured sample with the channel and without.

TABLE I: S_{11} Variations at 30 GHz for channelized and baseline designs.

	Magnitude (dB)	Phase (degrees)
Channelized	-0.277	168.23
Baseline	-0.138	166.31
Difference	-0.139	1.92

The simulation results reasonably predict the measured phase shift caused by the inclusion of the channel. Since the patches may not always be perfectly centered over the channels in a full reflectarray design, a simulation using Ansys HFSS with varying channel positions was conducted. The channel starts centered on the board and is stepped outward to the edge by 0.01 mm increments, reaching up to 1.8 mm from the center. The phase is recorded at 30 GHz for each point, as shown in Fig. 7. The results indicate that as the channel

position is moved, there is no significant change in the phase of the reflection, suggesting that the design will perform well in a full reflectarray configuration.

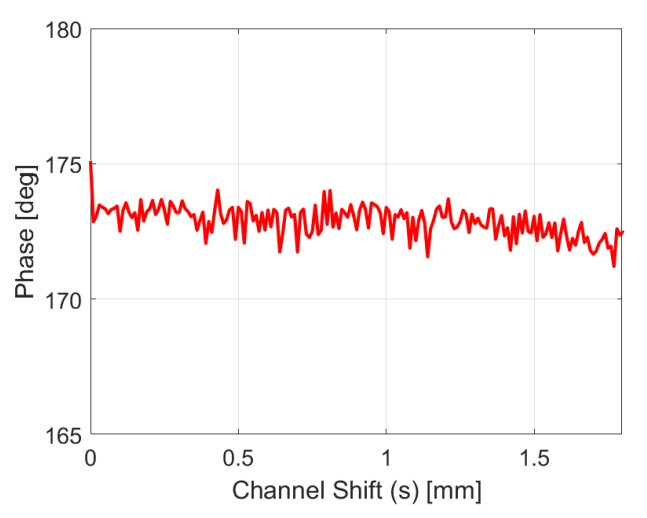


Fig. 7: Simulation of different channel placement.

VI. CONCLUSION

The results of this study demonstrate that the channelized structure introduced by the proposed hinge mechanism causes minimal disturbance to the reflectarray's electromagnetic performance, with phase variations measured to be within acceptable limits. This confirms that the hinge mechanism is viable from an RF standpoint and offers a promising solution for compact, deployable reflectarrays used in CubeSat and other space-constrained applications. Furthermore, the channel effects due to the Kevlar thread can be modeled ans simulated with Ansys HFSS, allowing for geometric changes to the structure to account for the small reflection phase variations when compared with the baseline design. The ability to reduce gaps between panels while maintaining structural rigidity and RF performance addresses a key challenge in folding reflectarrays. Future work should further explore the mechanical durability of the hinge in space environments, and investigate the scalability of the design for larger reflectarrays.

ACKNOWLEDGMENT

This material is based upon work supported by the National Science Foundation under Grant No. 1944599. The opinions, findings, and conclusions, or recommendations expressed are those of the authors and do not necessarily reflect the views of the National Science Foundation.

REFERENCES

- R. E. Hodges, D. J. Hoppe, M. J. Radway and N. E. Chahat, "Novel deployable reflectarray antennas for CubeSat communications," 2015 IEEE MTT-S International Microwave Symposium, Phoenix, AZ, USA, 2015, pp. 1-4,
- [2] A. J. Rubio, A. -S. Kaddour, C. Ynchausti, S. Magleby, L. L. Howell and S. V. Georgakopoulos, "A Foldable Reflectarray on a Hexagonal Twist Origami Structure," in IEEE Open Journal of Antennas and Propagation, vol. 2, pp. 1108-1119, 2021, doi: 10.1109/OJAP.2021.3127312.

- [3] A. J. Rubio, A. -S. Kaddour, H. Pruett, S. Magleby, L. L. Howell and S. V. Georgakopoulos, "A Deployable Volume-Efficient Miura-Ori Reflectarray Antenna for Small Satellite Applications," in IEEE Access, vol. 11, pp. 119313-119329, 2023, doi: 10.1109/ACCESS.2023.3327057.
- [4] S. V. Georgakopoulos et al., "Origami Antennas," in IEEE Open Journal of Antennas and Propagation, vol. 2, pp. 1020-1043, 2021, doi: 10.1109/OJAP.2021.3121102.
- [5] N. Miguélez-Gómez et al., "Thickness-Accommodation in X-Band Origami-based Reflectarray Antenna for Small Satellites Applications," 2020 IEEE International Conference on Wireless for Space and Extreme Environments (WiSEE), Vicenza, Italy, 2020, pp. 54-59, doi: 10.1109/WiSEE44079.2020.9262670.
- [6] J. Huang and J. A. Encinar, "Reflectarray antennas," IEEE Press, 2007
- [7] S. LeBlanc, K. Church, E. A. Rojas-Nastrucci, E. Martinez-de-Rioja, E. Carrasco and J. A. Encinar, "Advanced Manufacturing and Characterization of mm-Wave Two-Layer Reflectarray Cells," 2022 IEEE 22nd Annual Wireless and Microwave Technology Conference (WAMI-CON), Clearwater, FL, USA, 2022, pp. 1-4, doi: 10.1109/WAMI-CON53991.2022.978607
- [8] Rogers Corporation, "Radix™ Printable Dielectric 3D-Printable Dielectric Material for use on Fortify FLUX Series Printers," Radix datasheet, 2022.
- [9] J. O'Keefe, B. Roberts, B. Gray, K. Church and E. A. Rojas-Nastrucci, "An Additively Manufactured CPW-back-fed Wideband Circularly-Polarized Radix Metasurface Patch Antenna for X-Band Space Applications," 2023 IEEE International Conference on Wireless for Space and Extreme Environments (WiSEE), Aveiro, Portugal, 2023, pp. 19-22, doi: 10.1109/WiSEE58383.2023.10289327.